Turbulent Premixed Methane-Air Jet Flames: A Numerical Study

M. Chekired*, M.S. Boulahlib**, Z. Nemouchi*
*Laboratoire d'Energétique Appliquée et de Pollution
**Laboratoire d'Ingénierie des Transports et Environnement
University Mentouri-Constantine, Ain El Bey Road 25017, Constantine, Algeria

1 Introduction

Turbulent premixed combustion is projected to be one of the most attractive areas of research in recent decades. It is of a practical interest in different technical applications related to the well-known different energy systems such as spark-ignition engines, modern gas turbine, after burning process in jet engines and explosions in turbulent flows. To allow more reliable numerical predictions of the structures of such flames under a variety of practically relevant operating conditions of various combustion systems, sufficiently accurate models of combustion chemistry are needed. Using complex detailed chemistry in large-scale computations are currently impractical for reacting flows due to the large computational effort in calculations and other related numerical problems caused by the stiffness of the kinetics term [1]. The systematic reduction of detailed kinetic mechanisms to only a few kinetic steps represents a reasonable alternative approach that allow the study of the flame structure by asymptotic methods where the few kinetic parameters that mainly influence some of the properties of the flames such as the burning velocity or extinction strain rates are identified [2]. The research efforts has been more focused on premixed and non-premixed methane flames since the first mechanisms were derived in the mid-1980s, because the development of strategies that are useful in the systematic reduction of detailed kinetic mechanisms relay more on these flames that dedicated a good testing ground [3], [4], [5] , [6], [7], [8], [9]. In this study, we propose an application of a reduced scheme for methane combustion based on a two steps reduced mechanism proposed by N. Peters and F. A. Williams [6]. The experimental data of two turbulent premixed flames (Aachen flames) studied by Chen et al., [10] will constitute the main tool of comparison with our numerical calculations using RANS approach.

2 Governing Equations

KIVA II numerical code was considered in this study to perform numerical calculations. The governing equations of reacting flow are written using the same presentation of [11] with a specific modifications which were introduced into the code structure in order to allow a realistic representation of the studied problem. The numerical domain of interest is supposed to be two-dimensional and axis symmetric, extending up to 16.5 D$\times$4D (axial by radial direction). The numerical procedure used to solve the set of governing equations is described with detail in [11].

Correspondence to: chekired-mourad@hotmail.com

The continuity equation for species m:

$$\frac{\partial \rho_m}{\partial t} + div(\rho_m \vec{u}) = div\left[\rho D \nabla\left(\frac{\rho_m}{\rho}\right)\right] + \dot{\rho}^c{}_m$$

The continuity equation for the fluid mixture

$$\frac{\partial(\rho\vec{u})}{\partial t} + div(\rho\vec{u}) = 0$$

The momentum equation for the fluid mixture

$$\frac{\partial(\rho\vec{u})}{\partial t} + div(\rho\vec{u}\vec{u}) = -\nabla p - \nabla\left(\frac{2}{3}\rho k\right) + div\sigma + \rho\vec{g} \quad \text{Where: } \sigma = \mu\left[\nabla\vec{u} + \left(\nabla\vec{u}\right)^T\right] + \lambda div\vec{u} I d_3$$

The internal energy equation

$$\frac{\partial(\rho I)}{\partial t} + div(\rho\vec{u}I) = -p div\vec{u} + \rho\varepsilon - div\vec{J} + \dot{Q}^c, \; \vec{J} = -K\dot{\nabla}T - \rho D\sum_m h_m \nabla\left(\frac{\rho_m}{\rho}\right)$$

Turbulent kinetic energy equation

$$\frac{\partial(\rho k)}{\partial t} + div\left(\rho\vec{u}k\right) = -\frac{2}{3}\rho k div\,\vec{u} + \sigma : \nabla\vec{u} + div\left(\frac{\mu}{\Pr_k}\nabla k\right) - \rho\varepsilon$$

Dissipation turbulent kinetic energy equation

$$\frac{\partial(\rho\varepsilon)}{\rho t} + div\left(\rho\vec{u}\varepsilon\right) = -\frac{2}{3}C_{\varepsilon 1}\rho\varepsilon div\vec{u} + div\left(\frac{\mu}{\Pr_\varepsilon}\nabla\varepsilon\right) + \frac{\varepsilon}{k}\left(C_{\varepsilon 1}\sigma : \nabla\vec{u} - C_{\varepsilon 2}\rho\varepsilon\right)$$

$$C_{\varepsilon_1} = 1.44, C_{\varepsilon_2} = 1.92, \Pr_k = 1.0, \Pr_\varepsilon = 1.3 \qquad \mu = \mu_{air} + \rho C_\mu \frac{k^2}{\varepsilon}$$

Source terms due to chemistry are expressed using the following relations:

$$\dot{\rho}_m^c = W_m \sum_r \left(b_{mr} - a_{mr}\right)\dot{\omega}_r, \; \dot{Q}^c = \sum_r Q_r \dot{\omega}_r, \; Q_r = \sum_{m=1}^{nsp} \left(a_{mr} - b_{mr}\right)\left(\Delta h_f^0\right)_m$$

The State relations are assumed to be those of an ideal gas mixture

$$p = R_0 T \sum_m \frac{\rho_m}{W_m}, \; I = I(T) = \sum_m \frac{\rho_m}{\rho} I_m(T), \; C_p = C_p(T) = \sum_m \frac{\rho_m}{\rho} C_{p_m}(T), \; h_m = h_m(T) = I_m(T) + R_0 \frac{T}{W_m}$$

3 Combustion Chemistry Model

The complete kinetic scheme of methane combustion is represented using a two global steps scheme. This two step reduced mechanism was proposed by N. Peters and F. A.Williams [6]. and it is used to describe the reaction process in the flames, by which, the combustion of the intermediate species (H_2+αCO) is taken into account:

$$CH_4 + O_2 \rightarrow \frac{2}{\alpha+1}(H_2 + \alpha CO) + \frac{2\alpha}{1+\alpha}H_2O + \frac{1-\alpha}{1+\alpha}CO_2$$

$$O_2 + \frac{2}{\alpha+1}(H_2 + \alpha\, CO) \rightarrow \frac{2\alpha}{1+\alpha}H_2O + \frac{2\alpha}{1+\alpha}CO_2$$

The mean reaction rates of the chemical species in the flames are deduced from the complete kinetic scheme of methane combustion and are calculated using the following expressions:

$$\dot{\omega}_1 = k_{11}(T)[CH_4]K_{IV}^{\frac{1}{2}}(T)\frac{[O_2]^{\frac{1}{2}}[H_2]^{\frac{3}{2}}}{[H_2O]}\left[1 - \frac{k_{11}(T)}{k_1(T)}\frac{[CH_4]}{[O_2]}\right]^{\frac{1}{2}}, \; \dot{\omega}_2 = k_5(T)[O_2][M]K_{IV}(T)^{\frac{1}{2}}\frac{[O_2]^{\frac{1}{2}}[H_2]^{\frac{3}{2}}}{[H_2O]}\left(1 - \frac{k_5(T)[M]}{k_1(T)}\right)^{\frac{1}{2}}$$

The expressions for the different reaction-rate constants k_i, equilibrium constants K_J and the concentration of the third body M can be found in [6].

4 Problem Description and Inlet Boundary Conditions

The used burner design details for the experimental study of the two flames considered in this work are explicated by Chen and al. [10]. Global inlet conditions are summarized in Table 1 and a schematic illustration of the burner is represented on Fig. 1. The pilot flame is laminar, issuing from a surrounding coflow with a same diameter as well as the perforated plate and consisted of the same stoichiometric composition of the main flame.

Table 1: Global Inlet Conditions for the Two Flames

Flames	F1	F3
Re	52 000	24000
U_o (m/s)	65	30
k_o (m^2/s^2)	12.7	3.82

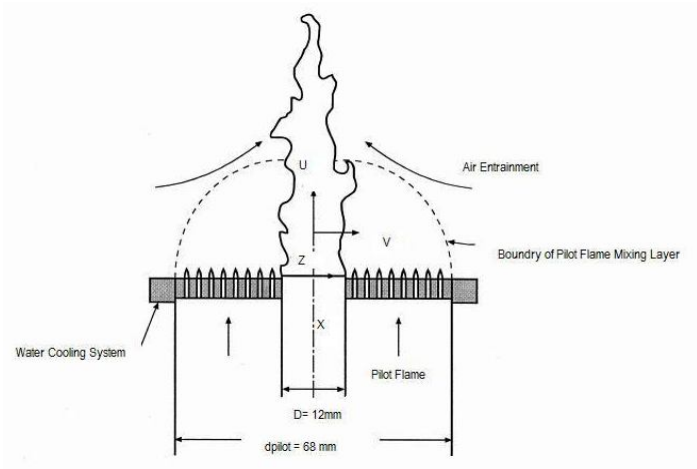

Figure 1. A schematic illustration of the burner [10].

5 Results and Discussions

The computational domain is consisted of 36×80 grid (axial by radial direction). Radial profiles at different axial positions in the flames F1, F3 of the mean axial velocity U normalized by the bulk velocity U_0, mean reaction progress variable and concentration of some major species are presented in Figures 2, 3, 4. Due to the gas expansion by combustion reaction, the mean axial velocity U is so broadening. One may observe the change of the velocity profile from the axial position Z/D=2.5 to 6.5 accompanied with the increase of U at almost radial positions x/D> 0.25D for the two flames. This thermal expansion causes the shear layer to be pushed outward in the radial direction.

The mean reaction progress variable c based on temperature is defined as $c = (T - T_u)/(T_b - T_u)$. T_b is the adiabatic flame temperature (T_b =2248K) and (T_u=298K) is the temperature of the fresh mixture at the exit of the burner. The F1 flame temperature is lower than that of F3 at the different stations in the flames; the fact that F1 has the faster the jet exit velocity, entrainment of ambient air into this flame is much significant. Along the axial positions, the increase of c in the flames is well reproduced by our calculations in a good agreement manner with experience and other works. The radial decrease in

calculated progress variable at different axial positions in the flames due to mixing with the ambient cold air is well captured by calculations. The slight difference between measured pilot flame temperature, our calculations and the other numerical studies could probably explain the discrepancies for F1 flame noted specifically in the pilot flame region at first axial position X/D=2.5 near to the burner exit. Other numerous works using different values of pilot flame temperature have noted these similar overpredictions [12], [13], [14].

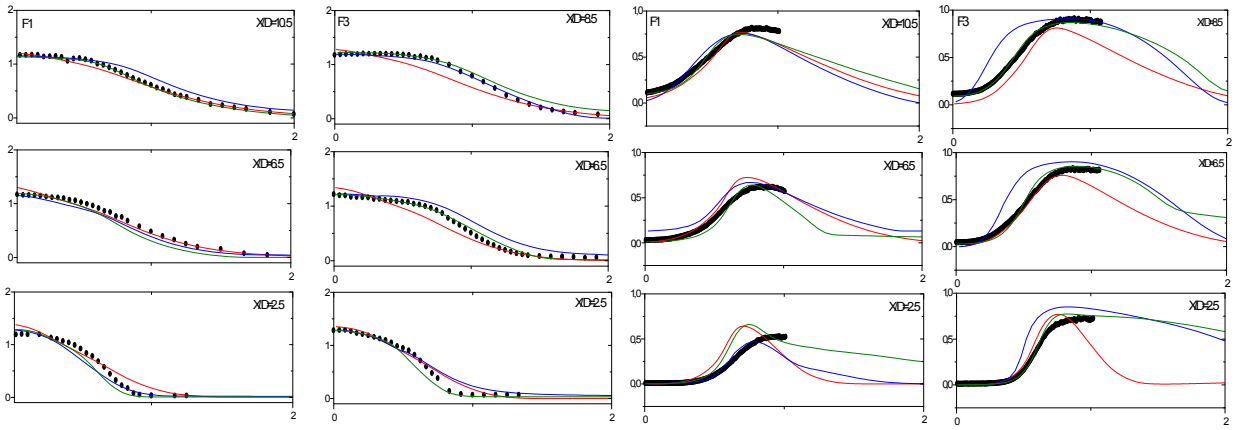

Figure 2. Radial distribution at different axial positions for the two flames. Left: Axial velocity U/U_0. Right: Mean reaction progress variable c. Symbols denotes experimental results, lines denotes numerical results: Red: Our numerical predictions, blue: [12], olive: [13].

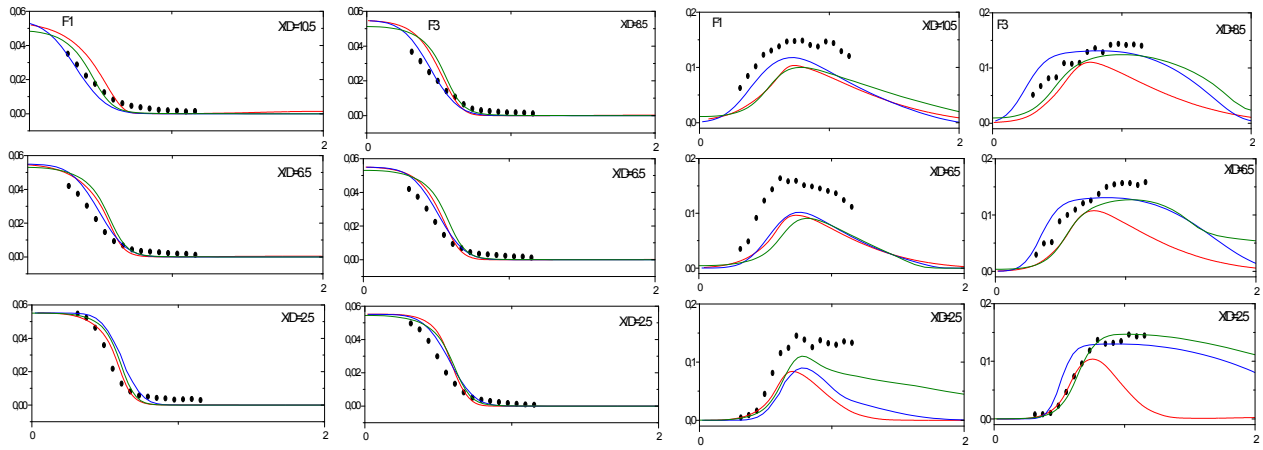

Figure 3. Radial distribution at different axial positions for the two flames. Left: CH_4 concentrations. Right: CO_2 concentrations. Symbols denotes experimental results, lines denotes numerical results: Red: Our numerical predictions, blue: [12], olive: [13].

For concentration profiles of some major species in the flames, CH_4 concentrations distribution shows a decreasing trend at the centerline as expected. On the burner axis the mean fuel consumption rate in the two flames agree well with [12] results but seems more slower than [13] in downstream positions specifically at axial positions X/D= 8.5 and10.5. For CO_2 concentrations radial profiles, a significant overall underprediction could be noted for F1 flame jointly with the other works. For this flame the calculated mean production rate of CO_2 increase slowly in agreement with experience. Our results agree well with those of [12] for the axial positions (2.5D and 6.5D) and with those of [13]. For the flame F3, the underprediction noted previously seems to be less significant specifically in the region

located between burner exit and the pilot flame and this is can be probably due to the relative good predictions of temperature distribution in the flame. It can be seen that the mean production rate of CO_2 is more dependant of the mean temperature distribution in the flames. Stöllinger [13] have noted the same CO_2 trend for F1 flame, arguing that it may be due to the slightly too high temperature levels predictions in these flames that imply high CO levels and a corresponding slower oxidation of CO to CO_2.

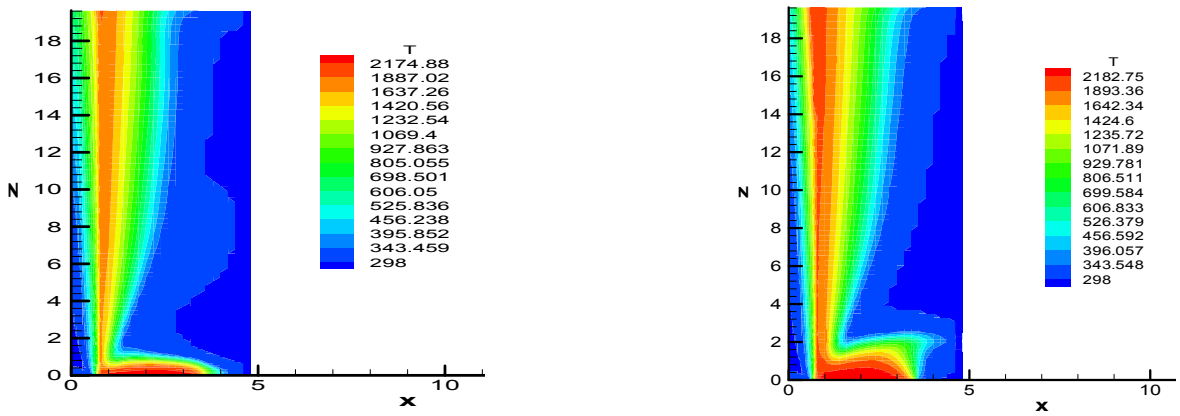

Figure 3. Temperature Contours in the Flames. Left: F1 Flame. Right: F1 Flame.

Acknowledgments: The authors would like to thank gratefully Pr. M. Gorokhovski of Ecole Centrale de Lyon (France) for his aid in using KIVA II code to perform numerical calculations.

References

[1] Skevis G et al. (2007). Understanding methane flame kinetics from reduced mechanisms. Int. J. Alternative Propulsion.1: 216-226.

[2] Peters N (1992). Fifteen lectures on laminar and turbulent combustion, Ercoftac Summer School, Aachen, Germany.

[3] Peters N, Rogg B (1993). Reduced kinetic mechanisms for applications in combustion system, Lecture notes in physics, Springer Verlag

[4] Peters N (1985). Numerical and asymptotic analysis of systematically reduced reaction schemes for hydrocarbon flames, Numerical Simulations of Combustion Phenomena, Lecture notes in physics, R. Glowinsky, B. Larrouturou and R. Temum (Eds.), Springer, Berlin. 241: 90–109.

[5] Peters N (1990). Systematic reduction of flames kinetics: principles and details, Fluid dynamical aspects of combustion theory, M. Onofri and A. Tesei (Eds.), Longman, New York. 232–246.

[6] Peters N, Williams F.A (1987). The asymptotic structure of stoichiometric methane-air flames. Combust. and Flam. 68: 185-207

[7] Peters N (1991). Reduced kinetic mechanisms and asymptotic approximations for methane-air flames, Lecture Notes in Physics, Smooke, M.D. (Ed.), Springer-Verlag, Berlin. 384: 48–67.

[8] Peters N, Kee R.J (1987). The computation of stretched laminar methane-air diffusion flames using a reduced four-step mechanism. Combust. and Flam. 68: 17–29.

[9] Smooke M.D (Ed.) (1991). Reduced kinetic mechanisms and asymptotic approximations for methane-air flames, Lecture Notes in Physics, Springer-Verlag, Berlin. 384:1–54.

[10] Chen Y-C and al. (1996). The detailed flame structure of highly streched turbulent premixed methane-air flames, Combust. and Flam. 107: 223-244.

[11] O'rourk A.A., P.J Butler, T.D. (1989) KIVA-II: A computer program for chemically reactive flows with sprays, Los Alamos Laboratory Report LA-11560-MS

[12] Heermann M (2006). Numerical simulation of turbulent bunsen flames with a level set flamelet model. Combust. and Flam. 145: 357-375.
[13] Stöllinger M, Heinz S (2007). PDF modeling and simulation of premixed turbulent combustion. Monte Carlo Meth. and Appli. 14: 343–377.
[14] Kolla H, Swaminathan N (2010). Strained flamelets for turbulent premixed flames II: Laboratory flame results. Combust.and Flam. 157: 1274-1289.

Nomenclature

ρ_m	: The mass density of species m.
$\dot{\rho}_m^c$	: Source term due to chemistry
ρ	: The total mass density
R_o	: The universal gas constant
W_m	: The molecular eight of species m
I_m	: The specific internal energy of species m
Cp_m	: The specific heat at constant pressure of species m
$C_{\varepsilon_1}, C_{\varepsilon_2}, C_\mu$	: Constants of the standard k–ε standard turbulence model
T	: The fluid Temperature
h_m	: The specific enthalpy for species m
$\dot{Q}_c$	: The source terms due to chemical heat release
k_i	: Constant reaction rates
k, ε	: The turbulent kinetic energy and its dissipation rate
Pr	: Prandtl number
Sc	: Schmidt number
J	: The heat flux vector
I	: The specific internal energy
g	: The specific body force
μ, λ	: The first and second coefficients of viscosity
σ	: The viscous stress tensor
P	: The fluid pressure
D	: The diffusion coefficient
$\dot{\omega}_{1,2}$	: The chemical production rates
x	: The molar fraction of species
K	: Heat conductivity coefficient
$\vec{U}$	: The fluid velocity